Electronic structure, chemical bonding, phase stability, and ground-state properties of $YNi_{2-x}(Co/Cu)_xB_2C$

P. Ravindran and B. Johansson
Condensed Matter Theory Group, Department of Physics, Uppsala University, Box 530, 75121 Uppsala, Sweden

O. Eriksson
Condensed Matter Theory Group, Department of Physics, Uppsala University, Box 530, 75121 Uppsala, Sweden
and Center for Materials Science and Theoretical Division, Los Alamos National Laboratory, Los Alamos, New Mexico 87545
(Received 7 July 1997; revised manuscript received 9 February 1998)

In order to understand the role of Ni site substitution on the electronic structure and chemical bonding in YNi_2B_2C, we have made systematic electronic-structure studies on YNi_2B_2C as a function of Co and Cu substitution using the supercell approach within the local density approximation. The equilibrium volume, bulk modulus (B_0) and its pressure derivative (B_0'), Grüneisen constant (γ_G), Debye temperature (Θ_D), cohesive energy (E_c), and heat of formation (ΔH) are calculated for $YNi_{2-x}(Co/Cu)_xB_2C$ ($x=0,0.5,1.0,1.5,2$). From the total energy, electron-energy band structure, site decomposed density of states, and charge-density contour we have analyzed the structural stability and chemical bonding behavior of YNi_2B_2C as a function of Co/Cu substitution. We find that the simple rigid band model successfully explains the electronic structure and structural stability of Co/Cu substitution for Ni. In addition to studying the chemical bonding and electronic structure we present a somewhat speculative analysis of the general trends in the behavior of critical temperature for superconductivity as a function of alloying. [S0163-1829(98)07525-0]

I. INTRODUCTION

Following the initial observation of superconductivity at 12 K in multiphase samples of $YNi_4B_xC_y$,[1] the superconducting composition has been identified[2] and a whole new class of layered intermetallic compounds of general formula RT_2B_2C (R=rare-earth, T=transition metal) has been discovered.[3] Considerable excitement was generated by the discovery of superconductivity in a number of such compounds,[4–6] and the interplay between superconductivity and magnetism in some of these systems.[7] This class of materials exhibits a variety of phenomena such as fairly high superconducting transition temperature (T_c) in RNi_2B_2C (R=Sc,Y,Lu),[1,2,4] coexistence of superconductivity, and magnetism in RNi_2B_2C (R=Ho,Er,Tm,Dy),[8–11,7] with remarkable double reentrant behavior in $HoNi_2B_2C$,[12] magnetic order in RNi_2B_2C (R=Nd,Sm,Gd,Tb),[13–15] valence fluctuations in $CeNi_2B_2C$ (Refs. 16,17) and UNi_2B_2C,[18] heavy fermion behavior in $YbNi_2B_2C$,[19] etc.

Although these materials have a layered-type crystal structure, suggesting that they may share the strongly anisotropic properties of the cuprates, band structure calculations[20–22] indicate that their electronic structure is much more three dimensional. Within this framework, superconductivity in these materials can be described by a conventional electron-phonon mechanism with relatively high transition temperatures due to a van Hove-like peak in the density of states (DOS) at E_F. In order to understand the correlation between superconductivity and electronic structure of YNi_2B_2C Lee *et al.*[23] made systematic investigations of the electronic structure for YNi_2B_2X (X=B, C, N, and O) using the LMTO method and found that a rigid-band-like shift of the Fermi level takes place, as the atom X is varied. From detailed band structure studies Mattheiss *et al.*[24] observed an energy band feature within the Ni-B-C s-p manifold which is sensitive to the NiB_4 tetrahedral geometry and the position of this key feature relative to E_F is mainly thought to be responsible for the superconductivity in these compounds. As the band structure calculations show the dominance of Ni-d character at the Fermi level for YNi_2B_2C,[20–22] substitution of Ni by its nearest neighbors in the periodic table, such as Co or Cu should give a better understanding about the metal-metal interactions and their role in electronic structure, superconductivity, and other transport properties. In contrast, the conduction electron contribution coming from the rare-earth site is rather small and hence, the effect of rare-earth ions on T_c comes mainly from the pair-breaking effect[7] through de Gennes scaling. Due to frequent experiments on superconducting and other properties of Co and Cu alloyed compounds one needs to understand the electronic properties, phase stability, and structural aspects of Co and Cu alloyed YNi_2B_2C. It is the purpose of this paper to answer some of these questions. We thus focus on the general trends in electronic structure and chemical bonding as a function of Co and Cu substitution and compare with available experimental results.

The replacement of Ni by Pd or Pt shows superconductivity where the mixed phase Y-Pd-B-C yields the highest T_c (23 K) in these systems.[5] The replacement of Ni by Co, Ir and Rh gives stable phases, but no superconductivity has been detected.[25] When Y is replaced with La another stable compound is obtained, $LaNi_2B_2C$, which is found to be nonsuperconducting. The absence of superconductivity in $LaNi_2B_2C$ is believed to be due to the increase of the Ni-Ni distance which reduces the Ni-Ni wave function overlap due to the large ionic radii of La compared with Y. In support of

the above view point, the 23 K superconductor YPd_2B_2C has a Pd-Pd distance of 2.652 Å and this value increases to 2.797 Å when Y is replaced with La. This reduces the T_c to 1.8 K.[26] From systematic studies of the superconducting behavior of RNi_2B_2C (R=Sc, Y, La, Lu, or Th) Lai *et al.*[18] found a correlation between the Ni-Ni distance and T_c with a maximum T_c for a Ni-Ni distance of 2.45 Å and the superconductivity completely disappears for a Ni-Ni distance of 2.683 Å. This result may indicates the importance of the Ni($3d$) dominated conduction band near E_F for the superconducting behavior of these materials.

Bonville *et al.*[27] measured T_c for $ErNi_2B_2C$ as a function of Co, Pd, or Pt substitution and found that T_c decreases ten times faster for Co substitution than for Pd or Pt substitution. They suggested that this difference may be due to a possible magnetic moment formation on the Co site in this material. Nagarajan *et al.*[28] found that 10 at. % Y replaced with Gd or 2.5 at. % Ni replaced with Fe decreases T_c of YNi_2B_2C by nearly the same amount. This indicates that the superconductivity in this material is more sensitive to Ni site substitution than to Y site substitution. Kadowaki *et al.*[29] measured T_c of $Y(Ni_{1-x}Co_x)_2B_2C$ as a function of x and found that the superconductivity is uniformly suppressed as a function of x with a rate of -0.64 K/at. % Co and that it disappears at $x \geqslant 0.20$. From the susceptibility measurements they concluded that the decrease of $N(E_F)$ is mainly responsible for the suppression of superconductivity. Bud'ko *et al.*[30] also made systematic studies of the influence of Ni site substitution with Co,Fe,Ru on the superconducting behavior of YNi_2B_2C and found a decrease of T_c with increasing the concentration of dopants. They arrived at the conclusion that the shift of Fermi energy (E_F) with changes in the valence electron concentration may be the primary cause for the suppression of superconductivity. Schmidt, Müller, and Braun[31] measured the superconductivity of the pseudoquarternary system $Y(Ni_{1-x}Co_x)_2B_2C$ and they found that the T_c value decreases from 15 K for the pure Ni compound to $T_c < 1.2$ K for $x > 0.2$. Gangopadhyay, Schuetz and Schilling[32] investigated the effect of substitution at the Ni site on T_c in $YNi_{2-x}(Co/Cu)_xB_2C$and found that T_c drops steeper for Co substitution ($dT_c/dx = -45.5$ K) than for Cu substitution ($dT_c/dx = -19.5$ K). From this observation they expected that either the peak in the DOS is asymmetric in energy, or that alloying affects both $N(E_F)$ and the electron-phonon coupling strength. In the past alloying the Ni atoms with Co and Cu has been done in order to give additional information about the superconducting properties of this interesting system. However, when alloying new issues arise, such as phase and structural stability. These issues may or may not be related to the superconducting properties.

The rest of the paper is organized as follows. The details about the construction of supercells and the computational method used in the present calculations are described in Sec. II. From the site decomposed DOS studies and the charge density analysis, the chemical bonding nature and the structural stability of YNi_2B_2C as a function of Co/Cu substitution are investigated in Sec. III. The experimentally observed changes in T_c by Co/Cu substitution is analyzed by our band structure results within the BCS formalism in Sec. IV. The results from our calculations are discussed in Sec. V. The important conclusions from our calculations are given in the last section.

II. STRUCTURAL ASPECTS AND DETAILS OF OUR CALCULATIONS

A. Crystal structure of YNi_2B_2C and construction of supercells

The crystal structure of YNi_2B_2C can be viewed as a filled variant of the $ThCr_2Si_2$ structure with the carbon atoms occupying the $2b$ position in the $I4/mmm$ lattice given in Table I. This structure can be simply visualized as NaCl type YC layers alternating with inverse PbO-type Ni_2B_2 layers in stoichiometry 1:1. Each Ni_2B_2 layer contains a square-planar Ni_2 array sandwiched between the boron plane with nickel atoms being tetrahedrally coordinated to four boron atoms. The NiB_4 tetrahedra are believed to be important for the superconductivity in this material. The shortest bond length is between B and C, which form a linear B-C-B unit with a nearest-neighbor distance (NND) of 1.55 Å. In the square planar Ni array, the NND of Ni-Ni atoms is 2.49 Å, which is close to that of Ni metal (2.50 Å) and the NND of Ni-B is 2.07 Å. The nearest-neighbor distances between Ni-Y and Ni-C atoms are both 3.17 Å. The crystal structure of YNi_2B_2C is depicted in Fig. 1(a), where the covalent bonding between boron and carbon as well as between nickel and boron are illustrated by bonds. In Fig. 1(a) the Ni_2B_2 layers are connected by short boron-carbon covalent bonds. Due to this strong covalent bond, the calculated band structures are found to have three-dimensional character,[20,21,33,22] despite the fact that the structure looks similar to a layered material.[3,34]

The simple way of constructing a supercell in a $I4/mmm$ lattice is to assume a primitive tetragonal lattice with space group $P4/mmm$ instead of a body centered tetragonal (bct) lattice. This is equivalent to adding one additional cell in the z direction of the primitive cell of the bct lattice. According to the symmetry of the $P4/mmm$ lattice, the Y atoms will be in $1a$ and $1d$ positions, the Ni atoms will be in the $4i$ position, the B atoms will be in $2g$ and $2h$ positions, and the C atom will be in the $1a$ as well as $1c$ positions. As all the four Ni atoms are in the same equivalent position, this supercell does not fit our requirement. From a chemical picture, if we substitute Co/Cu for some of the Ni atoms in YNi_2B_2C, the Ni atoms closer to the substituent will behave differently than the others. This requires that we construct a supercell in the $P\bar{4}m2$ lattice with atom positions given in Table I, since then it is possible to treat all the four Ni atoms independently. It should be noted that the boron atoms which have only one position type in the primitive cell have two different inequivalent positions in the supercell, depending upon their position parameter z given in Table I. As a result there are 12 atoms of 8 different types involved in our supercell calculations.

For the supercell calculation we have constructed two types of cells. First we have calculated the minimum energy configuration of the supercells by comparing different crystallographic sites for the Co and Cu substitution. Further details about these calculations are described later. From this study, the constructed first supercell is of $Y_2Ni_3CoB_4C_2$ type

TABLE I. The structural parameters for YNi_2B_2C and the supercell used in the present calculations. The boron atoms in the supercell are in two equivalent $2g$ positions with different z values. To distinguish these two boron atoms we have represented them by $(2g)$-a and $(2g)$-b. The lattice parameters are in Å.

System YNi_2B_2C	$Z=2$	Space group $I4/mmm$ (No. 139)	Pearson symbol $tI12$	
Lattice Parameters	$a=3.526$	$b=10.538$	$c/a=2.9886$	
Atom	Position	x	y	z
Y	$2a$	0.0	0.0	0.0
Ni	$4d$	0.0	0.5	0.25
B	$4e$	0.0	0.0	0.353
C	$2b$	0.0	0.0	0.5
System $Y_2Ni_3CoB_4C_2$	$Z=2$	Space group $P\bar{4}m2$ (No. 115)	Pearson symbol $tP12$	
Lattice Parameters	$a=3.5245$	$c=10.504$	$c/a=2.9802$	
Atom	Position	x	y	z
Y	$2g$	0.5	0.0	0.75
Ni(1)	$1d$	0.0	0.0	0.5
Ni(2)	$1a$	0.0	0.0	0.0
Ni(3)	$1b$	0.5	0.5	0.0
Co	$1c$	0.5	0.5	0.5
B(1)	$2g$-a	0.5	0.0	0.103
B(2)	$2g$-b	0.5	0.0	0.397
C	$2g$	0.5	0.0	0.25

[see Fig. 1(b)], where we have substituted the Co atom at the $1d$ position and the three Ni atoms are occupying the $1a$, $1b$, and $1c$ positions given in Table I. The second one is of $Y_2Ni_2Co_2B_4C_2$ type [see Fig. 1(c)], where the two Ni atoms occupy the $1b$ and $1c$ positions and two Co atoms the $1a$ and $1d$ positions given in Table I. For $YCo_3NiB_4C_2$ we have just interchanged the Co and Ni atoms in the first structure type. However, we have used the same positions as given in Table I for B, Y, and C in all our supercell calculations. For Cu substitution, we have replaced the Co atom by Cu in the above mentioned supercells. At the theoretical equilibrium volume in $Y_2Ni_3CoB_4C_2$, each Co($1d$) atom is surrounded by four boron atoms $(2g-b)$ as nearest neighbors at a distance of 3.952 a.u. and 4 Ni atoms $(1d)$ as second nearest neighbors at 4.763 a.u. The c/a values for our calculations are taken from the experimental studies.[32,29] However, for higher Cu substitutions no experimental lattice parameters are available due to that metastability then arises. Hence we have extrapolated the c/a values from the available experimental values and they are given in Table II.

B. Computational details

For solving the one-electrons Schrödinger-like equation self-consistently we have used the scalar-relativistic linear muffin-tin (LMTO) orbital method in the atomic sphere approximation (ASA) including the combined correction terms.[35] In ASA the choice of sphere radii is important, in particular for the open structures such as that of YNi_2B_2C. Because of the layered nature of the crystal structure Coehoorn[33] introduced empty spheres in the $4(e)$ position (0,0,0.225) in the $I4/mmm$ lattice in oreder to fill space with spheres in a close packed manner. If one uses the Wiegner-Seitz radii given in Tables II and III, without an empty sphere addition, the overlap volume of the atomic spheres is less than 9% of the permissible limit of the use of the ASA.

The basis set consists of Y $5s$, $4d$, Ni(Co,Cu) $4s$, $4p$, $3d$, and boron, as well as carbon $2s$ and $2p$ LMTO's. The Y $5p$, $4f$, and boron as well as carbon $3d$ partial waves were included in the tails of the above mentioned LMTO's. The basis functions were calculated at fixed energies E_ν which were chose to be at the center of gravity of the occupied parts of the site and angular momentum projected bands. The core states are treated relativistically, while the valence states were calculated scalar relativistically, i.e., except for the spin-orbit coupling all the other relativistic effects were incorporated. The tetrahedron method for the Brillouin zone (i.e., k space) integrations was used in its latest version (Blöchl *et al.*[36]), which avoids misweighing and corrects errors due to the linear approximation of the bands inside each tetrahedron. We have used 447 k points in the irreducible wedge of the first Brillouin zone (IBZ) of the bct lattice for our conventional cell calculations and 333 k points in the IBZ of the simple tetragonal lattice for our supercell calculations. The von Barth–Hedin parametrization is used for the exchange correlation potential within the local density approximation. The self-consistency iterations are continued until the total energy difference between two consecutive iterations is less than 10^{-6} Ry/f.u.

In order to check the reliability of our ASA calculations, we have also used the all-electron full-potential linear muffin-tin orbital (FPLMTO) method[37] for the calculation of the equilibrium volume of YNi_2B_2C and YCo_2B_2C. In the FPLMTO method, no shape approximation is made to the potential and the charge density; the warping terms in the

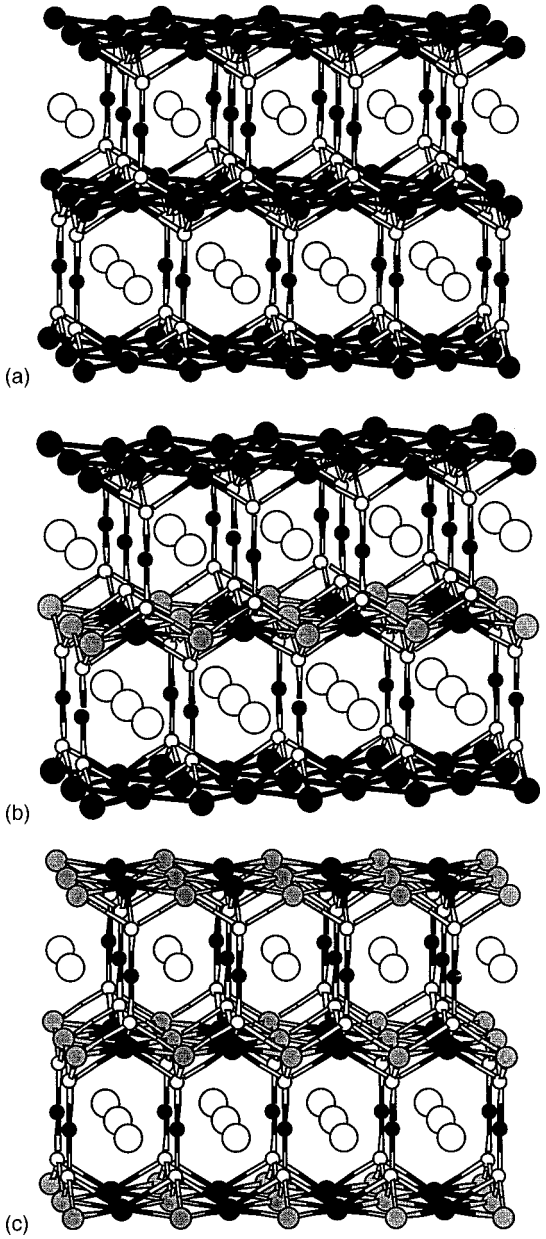

FIG. 1. The crystal structures of $YNi_{2-x}(Co/Cu)_xB_2C$. (a) YNi_2B_2C, (b) $YNi_{1.5}(Co/Cu)_{0.5}B_2C$, and (c) $YNiCoB_2C$. The big black circles represent Ni, the small black circles represent C, the big white circle is Y, and the small white circle represents the boron atoms. The grey circles denote the substituent Co/Cu atoms. The transition metal and boron atoms as well as the boron and the carbon atoms are connected by bonds.

interstitial region and the nonspherical contribution at the nuclei sites are explicitly taken into account. The density and potential are expanded in cubic harmonics inside nonoverlapping muffin-tin spheres and in a Fourier series in the interstitial region. Spherical harmonic expansions were carried out through $l_{max}=8$ for the bases, potential and charge density. The exchange and correlation potential was treated using the generalized gradient approximation (GGA) as proposed by Perdew and Wang.[38] The basis set was comprised of augmented linear muffin-tin orbitals.[35] The tails of basis function outside their parent spheres were linear combinations of Hankel or Neumann functions with nonzero kinetic energy. The basis contains $4s$, $5s$, $4p$, $5p$, $4d$, and $4f$ orbitals of yttrium, $4s$, $3p$, $4p$, and $3d$ orbitals of nickel, and $2s$, $2p$, and $3d$ orbital of boron and carbon. All orbitals were contained in the same energy panel, with the $4s$ and $4p$ of Y and $3p$ of Ni/Co were treated as a pseudovalence state in an energy set which is different from the rest of the basis function. Further, we used a so-called ''double basis'' where we used two different orbitals of l,m_l character each connecting, in a continuous and differential way, to Hankel or Neumann functions with different kinetic energy. The integration over the Brillouin zone is done using the special point sampling[39] with a Gaussian width of $\sim$10 mRy. We have used 75 k points in the IBZ for our self-consistent calculations.

TABLE II. The Wigner Seitz radii for the atomic spheres (in a.u) corresponding to the theoretically obtained equilibrium volumes (V_0 in a.u^3/f.u.) and c/a for $YNi_{1.5}Co_{0.5}B_2C$ [A, where $T(1d)$ Co], $YNiCoB_2C$ [B, where $T(1d,1a)$ Co], $YNi_{0.5}Co_{1.5}B_2C$ [C, where $T(1a,1b,1c)$ Co], $YNi_{1.5}Cu_{0.5}B_2C$ [D, where $T(1d)$ Cu], $YNiCuB_2C$ [E, where T($1d$,$1a$) Cu], and $YNi_{0.5}Cu_{1.5}B_2C$ [F, where $T(1a,1b,1c)$ Cu] used in the present calculations.

Parameter	A	B	C	D	E	F
V_0	455.434	449.751	447.973	459.482	464.179	467.996
c/a	2.980	3.007	3.017	3.003	3.007	3.017
Y	3.765	3.737	3.728	3.766	3.777	3.783
$T(1d)$	2.741	2.731	2.711	2.701	2.711	2.800
$T(1a)$	2.732	2.731	2.720	2.742	2.711	2.759
$T(1b)$	2.732	2.714	2.720	2.742	2.792	2.759
$T(1c)$	2.724	2.714	2.728	2.782	2.792	2.719
$B(1)$	1.686	1.696	1.700	1.706	1.714	1.725
$B(2)$	1.686	1.696	1.700	1.706	1.714	1.725
C	1.699	1.708	1.711	1.718	1.726	1.736

C. Calculation of ground state properties

1. Structural disorder effect

Both Co and Cu are chemically closer to Ni than Y, B, or C. Hence, it is expected that Co/Cu will prefer to occupy the Ni site in YNi_2B_2C. As mentioned above, the Ni atoms in the supercells occupy four inequivalent sites such as $1a$, $1b$, $1c$, and $1d$. In order to understand the site occupancy of Co/Cu in YNi_2B_2C we have performed total energy calculations for $Y_2Ni_3(Co/Cu)B_4C_2$ by substitution of Co/Cu in the $1a$, $1b$, $1c$, and $1d$ positions. From this study we found that the total energy is almost the same, irrespective of the abovementioned four sites of Co or Cu occupation in $Y_2Ni_3(Co/Cu)B_4C_2$ and $Y_2(Co/Cu)_3(Ni)B_4C_2$ supercells.

TABLE III. The Wigner-Seitz radii for the atomic spheres (in a.u) corresponding to theoretically obtained equilibrium volumes (V_0 in a.u.^{3}/f.u.) and c/a for YCo_2B_2C, YNi_2B_2C, and YCu_2B_2C used in the present calculations.

Compound	V_0	c/a	Y	Ni/Cu/Co	B	C
YCo_2B_2C	446.195	3.026	3.719	2.717	1.704	1.715
YNi_2B_2C	455.967	2.988	3.763	2.734	1.692	1.705
YCu_2B_2C	471.817	3.026	3.789	2.768	1.736	1.746

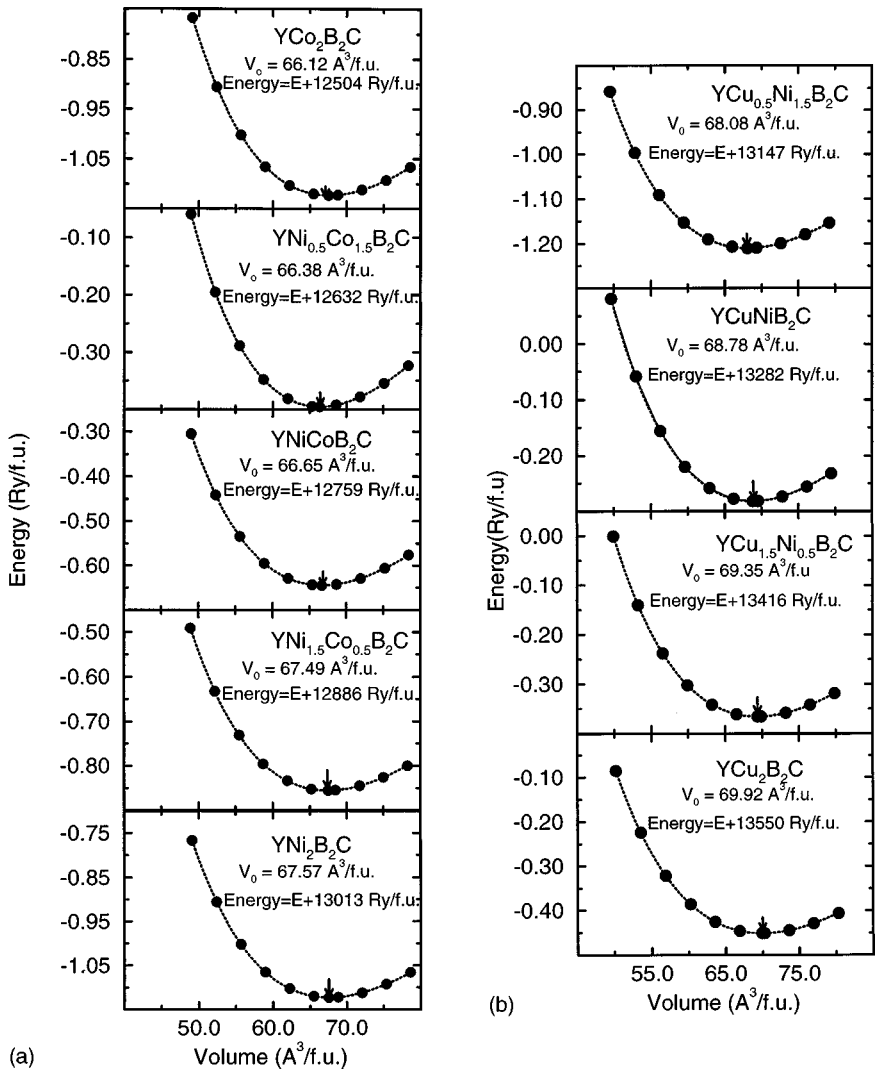

FIG. 2. The total energy versus volume curves for (a) $YNi_{2-x}Co_xB_2C$ and (b) $YNi_{2-x}Cu_xB_2C$. The equilibrium volumes are indicated by arrows. The total energies are scaled through the corresponding energies given in each figure.

However, in the case of $Y_2Ni_2(Co/Cu)_2B_4C_2$, from all six possible combinations of atomic arrangement, we have found that the affinity of Co or Cu towards Ni is larger than the Co-Co or Cu-Cu attraction. In other words, our calculations show that the total energy of $Y_2Ni_2(Co/Cu)_2B_4C_2$ with separated Ni_2B_2 and $(Co/Cu)_2B_2$ layers is around 10 mRy/f.u. higher in energy than that with $[Ni(Co/Cu)]_2B_2$ layers. For this reason, we have in the calculations to be discussed below used the supercell which has an alternative layer of Ni is replaced by Co/Cu as shown in Fig. 1(c). However, we note that the energy difference between Co or Cu substitution on different sites is quite small compared to the properties we are interested in here, i.e., change in electronic structure, equilibrium volume, and cohesion due to Co/Cu substitution.

2. Equilibrium properties

The total energy as a function of volume for $YNi_{2-x}Co_xB_2C$ and $YNi_{2-x}Co_xB_2C$ is plotted in Figs. 2(a) and 2(b), respectively. From the minimum in these total energy curves the equilibrium volume as a function of Co/Cu substitution is derived and shown in Fig. 3. To check the reliability of our ASA results, we have repeated our total energy studies of YNi_2B_2C and YCo_2B_2C using the general-

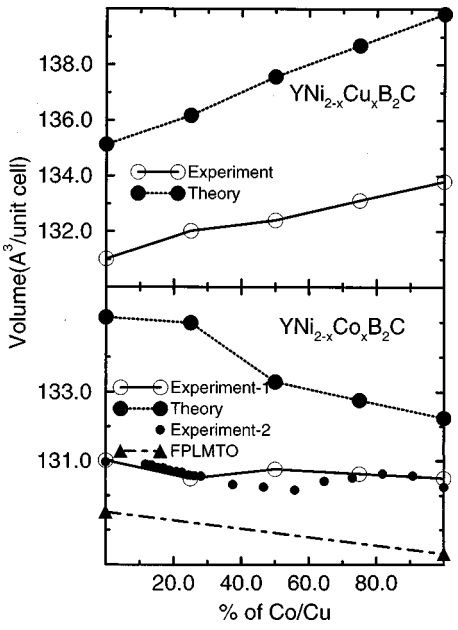

FIG. 3. The calculated equilibrium volumes for YNi_2B_2C as a function of Co/Cu substitution. The experimental open circles were reported by Gangopadhyay *et al.* and the experimental closed circles were reported by Kadowaki *et al.*

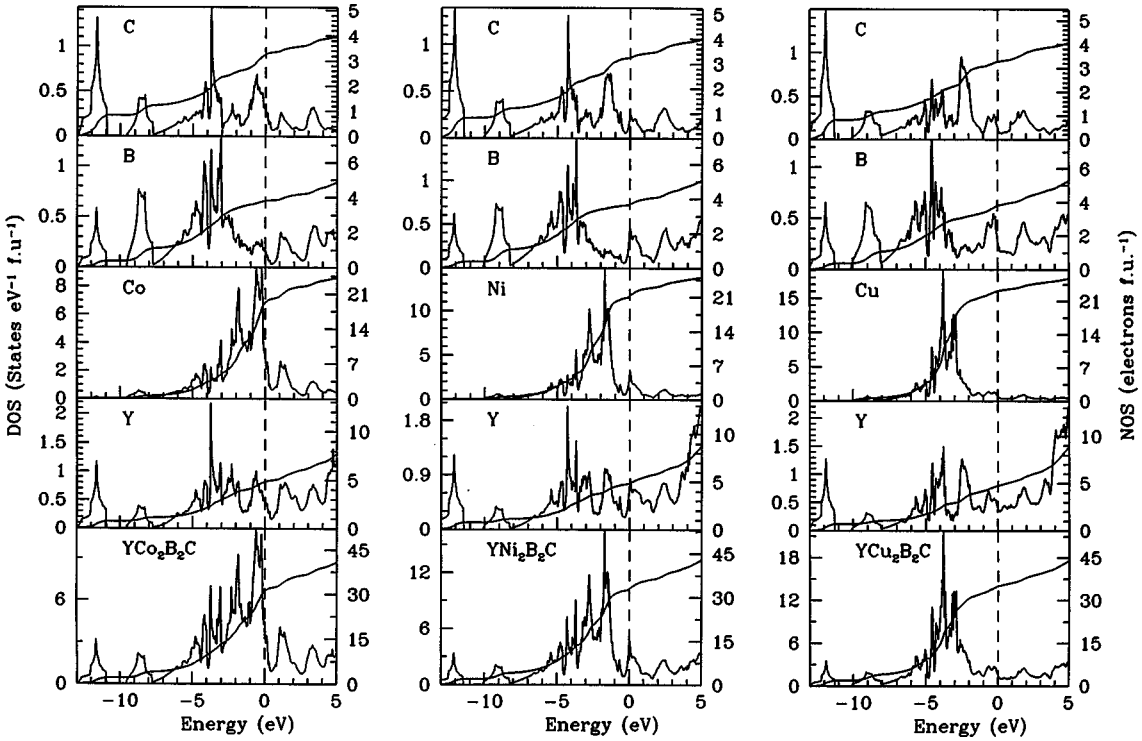

FIG. 4. The total and site projected density of state for YT_2B_2C (T=Co, Ni , or Cu). The dashed line denotes E_F.

ized gradient corrected full-potential LMTO method. Our full-potential results, shown in Fig. 3, underestimate the equilibrium volume with 1.1% for YNi_2B_2C and 1.7% for YCo_2B_2C. The ASA calculations overestimate the equilibrium volume with 3.1% for YNi_2B_2C and 1.3% for YCo_2B_2C. Generally the LDA underestimates the equilibrium volumes and hence, the overestimation of equilibrium volume is due to a limitation of the use of ASA. However, what is important to note is that both ASA and full-potential calculations are able to reproduce the experimental trend. For this reason it seems safe to draw conclusions from the TB-LMTO calculations about the changes in the chemical bonding due to Co/Cu alloying. Further, the overall topology of the DOS curves for YNi_2B_2C and YCo_2B_2C obtained from our FPLMTO calculations is very similar to those obtained from our ASA calculations. We have also calculated the c/a changes in YNi_2B_2C as a function of volume in the FPLMTO method. Our calculations show that a 5% decrease in volume increase the c/a with 0.48% only. This shows that the assumption of using the experimental c/a in our supercell calculations will not affect considerably the properties studied here, and our conclusion about equilibrium volume and bulk modulus, to be discussed below, are reliable.

III. CHEMICAL BONDING AND STRUCTURAL STABILITY FROM DOS STUDIES AND CHARGE DENSITY ANALYSIS

A. DOS studies

Due to the presence of strong covalent hybridization between the transition metal (TM) nontransition metal (NM) valence orbitals in binary compounds, a deep valley in the vicinity of E_F called a pseudogap has often been observed.[40,41] There appears to be strong correlation between stability and the position of the Fermi level with respect to the pseudogap in the DOS curve for binary alloys; that is, if E_F falls within this pseudogap region, which separates bonding states from the antibonding-nonbonding states in a particular structure, the system will be more stable.[41] In fact this type of behavior is partly the reason for why simplified models, such as the structural energy difference theorem[42] work. The total DOS given in Fig. 4 illustrates that YCo_2B_2C as well as YNi_2B_2C have a pseudogap and that this feature has disappeared in YCu_2B_2C.

It is well established that the bonding nature of solids can be usefully illustrated by partial density of state analysis.[43] In order to understand the electronic structure and bonding behavior of YNi_2B_2C as a function of Co/Cu substitution the site projected density of states of YT_2B_2C (T=Co,Ni,Cu) are given in Fig. 4. The DOS curve of YCo_2B_2C to the left in Fig. 4 shows that most of the atom projected DOS overlap over a large energy range. This illustrates the existence of strong covalent bonding between Y, Co, B, and C. Let us for simplicity now consider the Co d states, the Y d states, B p states, and C p states as one degenerate energy band which can contain a total of 48 electrons. Half of these states are bonding whereas the other half are antibonding. In YCo_2B_2C there are approximately 23.5 electrons/f.u. whereas in YNi_2B_2C there are approximately 25.5 electrons/f.u. in the valence band. This illustrates that almost all the bonding states are filled in YCo_2B_2C whereas some antibonding states are filled in YNi_2B_2C. This is consistent with the lower equilibrium volume of YCo_2B_2C and the higher cohesive energy. The DOS curve of YCo_2B_2C given in Fig. 4 shows that the pseudogap is 0.5 eV away from the Fermi level (i.e., E_F lies within the bonding states). This is consistent with the discussion above and indicates that not all the bonding states are filled. For YNi_2B_2C the pseudogap is below E_F and anti-

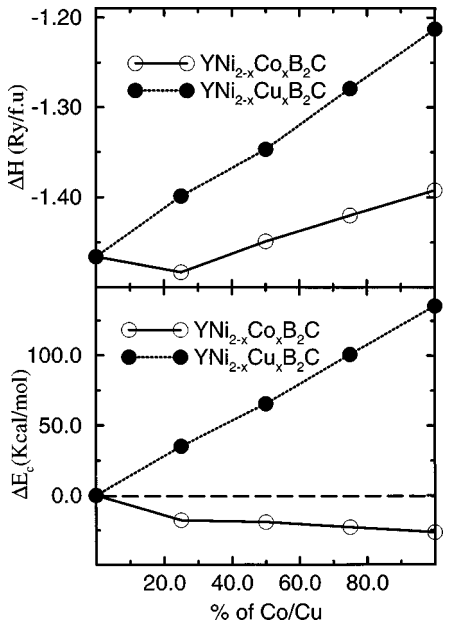

FIG. 5. The heat of formation (ΔH) and cohesive energy (ΔE_c) for $YNi_{2-x}(Co/Cu)_xB_2C$. The cohesive energy for YNi_2B_2C has been set equal to zero.

bonding states are occupied. From our DOS analysis we conclude that a maximum bonding is found for $YNi_{1.12}Co_{0.88}B_2C$.

It is interesting to note that E_F falls on a peak in the DOS curve in the superconducting YNi_2B_2C and that this feature appears neither in the nonsuperconducting YCo_2B_2C nor in YCu_2B_2C. It should be mentioned that this kind of peak structure in the vicinity of E_F has been observed for conventional high-T_c superconductors such as transition metal compounds with structure $A15$, $L1_2$, $E2_1$, etc.[44,45,22] Our angular momentum (not shown here) and site decomposed DOS for YCu_2B_2C shows that the Cu-3d states are almost filled and also that E_F falls on the antibonding region of the DOS curve (see DOS of YCu_2B_2C in Fig. 4). Hence, the covalent interaction between Cu and B is much weaker than for Ni-B and Co-B. This is most likely the explanation for the fact that YCu_2B_2C has not been found experimentally.[32]

In order to understand the structural stability and bonding behavior of YNi_2B_2C as a function of Co/Cu substitution the cohesive energy of $YNi_{2-x}Co/Cu_xB_2C$ is shown as a function of x in Fig. 5. The cohesive energy of YNi_2B_2C is the reference level and is set to zero. From Fig. 5 it is clear that the bond strength increases with Co substitution and decreases with Cu substitution. Consistent with the above conclusion, the calculated value of the heat of formation (see Fig. 5) for Co substituted systems is more negative than for YNi_2B_2C as well as for Cu substituted systems. Further, the increase trend of the bulk modulus and Debye temperature by Co substitution discussed later also indicates the increase of bond strength.

In order to understand the changes in the electronic structure as a function of Co/Cu substitution in YNi_2B_2C we show the site projected density of states of $YNi_{2-x}Co_xB_2C$ in Fig. 6. In $YNi_{1.5}Co_{0.5}B_2C$, each Co atom is surrounded by four

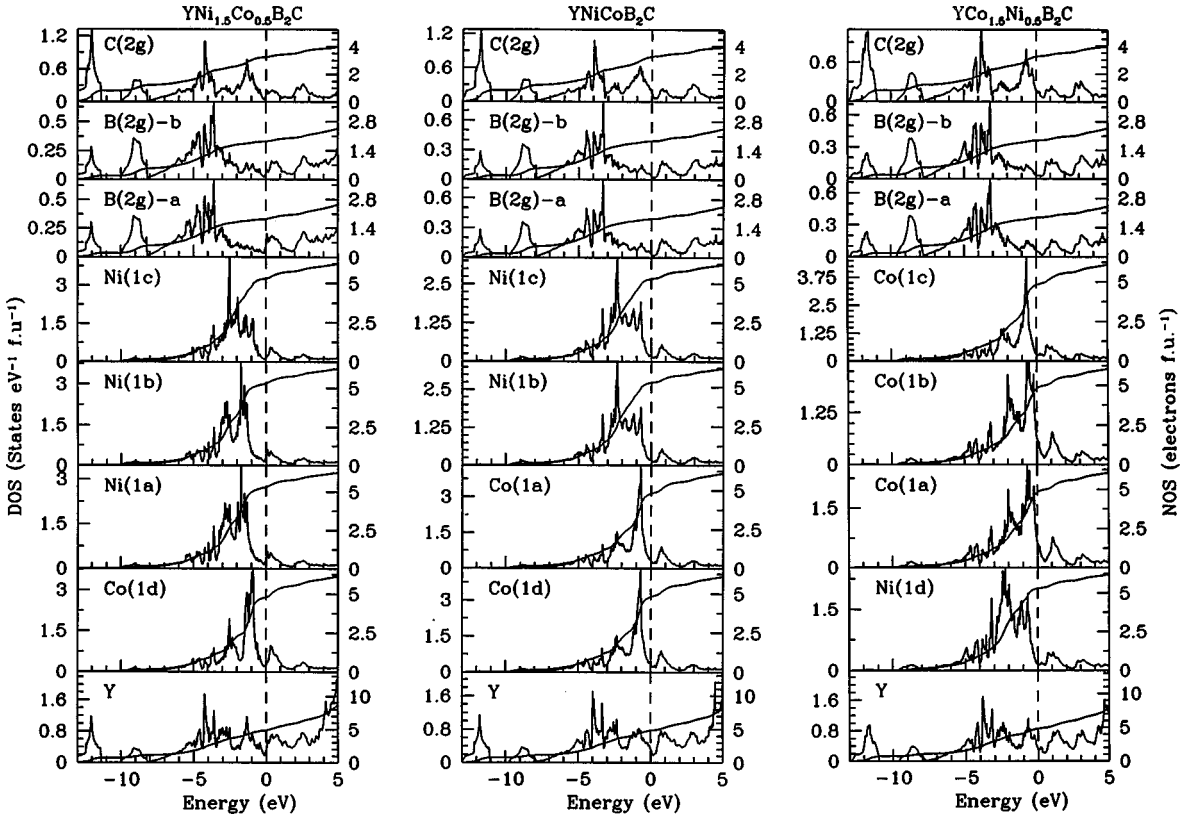

FIG. 6. The site projected density of state of $YNi_{2-x}Co_xB_2C$ ($x=0.5,1,1.5$). The dashed line denotes E_F. The atom positions 1a, 1b, etc. are the same as given in Table I.

B($2g$-b) atoms as nearest neighbors and four Ni($1c$) atoms as next-nearest neighbors. From this figure it is clear that the boron atoms closer to Co are behaving different from those which are closer to Ni atoms in $YNi_{1.5}Co_{0.5}B_2C$. The site decomposed DOS in Fig. 6 also shows that E_F falls within a pseudogap region in the DOS curve for boron atoms closer to Co and that E_F falls on a peak of the DOS for boron atoms closer to Ni. Further more, the spectral weights are transformed to the lower energy side in the DOS of B($2g$-a) compared to B($2g$-b). Even though the Ni($1c$) atoms are present as next-nearest neighbors at a distance of 2.5204 Å from Co, the DOS is affected significantly by the interaction with Co. In particular, the DOS of Ni($1a$ and $1b$) are much narrower than that of Ni($1c$). Further, E_F falls in a pseudogap region in both Co($1d$) and Ni($1c$) in $YNi_{1.5}Co_{0.5}B_2C$ which indicates that there is a strong covalent hybridization between Ni($1c$) and Co($1d$) compared with that between Ni($1a$) and Ni($1b$). Due to the equal number of Co and Ni in $YNiCoB_2C$ the bonding between the transition metals is more homogeneous than that in $YNi_{1.5}Co_{0.5}B_2C$. As a result, the local DOS of nickel in two inequivalent sites is similar to each other. It is of course obvious that the number of Co-Ni bonds in $YNiCoB_2C$ is larger than in $YNi_{1.5}Co_{0.5}B_2C$. As mentioned above the Co-Ni bonds show a more stronger covalent hybridization than Ni-Ni, the pseudogap in the DOS curve of $YNiCoB_2C$ is much more pronounced than that of $YNi_{1.5}Co_{0.5}B_2C$. Similar to $YNi_{1.5}Co_{0.5}B_2C$, the Co($1c$) and Ni($1d$) DOS in $YNi_{0.5}Co_{1.5}B_2C$ also has the E_F falling on a pseudogap. But, due to the decrease of e/a (electron per atom) ratio, the E_F in Co($1a$) and Co($1b$) falls to the shoulder of the main d DOS in $YNi_{0.5}Co_{1.5}B_2C$.

Similarly we have analyzed the changes in DOS of YNi_2B_2C as a function of Cu substitution. Due to the almost filled nature of the Cu-3d state in $YNi_{1.5}Cu_{0.5}B_2C$ the DOS of Ni closer to Cu has not changed much (not shown here) compared with Ni closer to Co in $YNi_{1.5}Co_{0.5}B_2C$. Our calculations show that instead of an hybridization effect, the shift in E_F is more important to explain the changes in physical properties by Cu substitution.

B. Charge density analysis

The main types of chemical bonding in YNi_2B_2C are analyzed with the help of Figs. 7(a) and 7(b); where valence charge density maps in the 001 plane [Fig. 7(a)], i.e., the Y-C layers and the plane parallel to the z axis [Fig. 7(b)] are shown. The contours shown in Figs. 7 are from ASA calculations but the full potential calculations give similar contours. From Fig. 7(a) we notice that the charge density is essentially spherical around the different atoms, with small covalent features and together with our calculated occupation numbers we conclude that the bonding between Y and C is dominantly ionic. This result is consistent with the recent core level energy measurements.[46] The observed ionic nature of the bonding between Y-C is reasonable because the Pauling electronegativity difference between Y and C is quite large $\sim$1.2. Moreover, a finite nonspherical charge density (covalent) distribution exists between Y and C. Hence, the bonding between Y and C has a dominant ionic character with a small degree of covalency. The special feature of Fig. 7(b) is the presence of strong directional bonding between the boron and carbon atoms connecting the two Ni_2B_2 layers above and below. Hence, carbon plays an important role for the stability of this system. This may be the reason why a synthesis of the noncarbide YNi_2B_2 has not been successful. Further, from Fig. 7(b) it is also seen that the covalent character in the bonding between nickel and boron is clear. This is consistent with interpretation of photoemission[47] and x-ray absorption[48] measurements. The existence of covalent bonding between Ni, B, and C has also been confirmed very recently by high resolution core electron spectroscopy studies.[49]

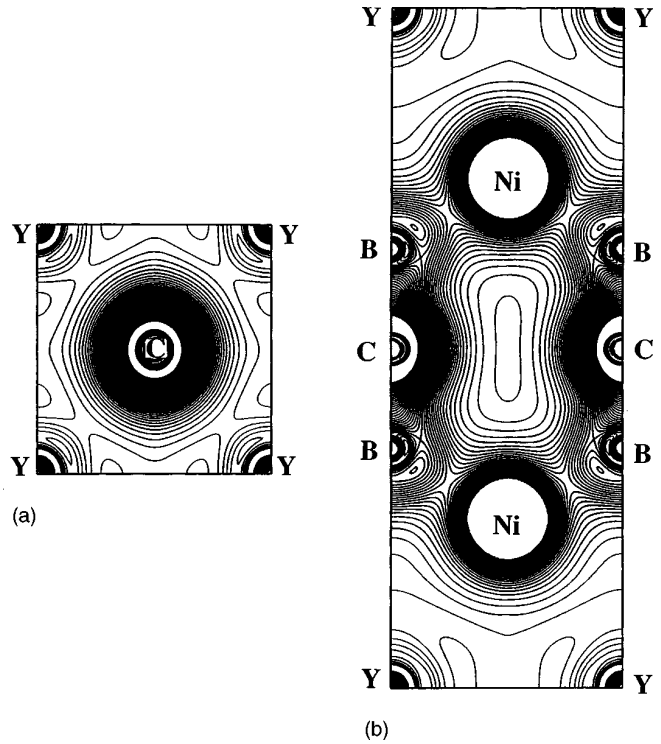

FIG. 7. The valence charge density for YNi_2B_2C in (a) 001 plane and (b) 100 plane. 50 contours are drawn between 0.01 and 0.25 electrons/a.u^3.

In order to understand the role of the Co/Cu substitution on the bonding behavior of YNi_2B_2C, the valence band charge density for YT_2B_2C (T=Co,Ni,Cu) around 1 eV near the Fermi level is given in Fig. 8. From this figure it is clear that there is a strong directional bonding between Co and B which is reduced for Ni-B and Cu-B. Our calculations thus show that the bond strength between the transition metal and boron atoms decreases in the order Co-B $>$ Ni-B $>$ Cu-B and this is consistent with the bond order obtained from an embedded-cluster approach by Zeng *et al.*[50] The site decomposed DOS given in Fig. 4 clearly shows that the Cu 3d states are almost filled in this compound. This is one of the reasons why the covalent bonding between Cu-B is weaker than that of Ni-B as well as that of Co-B. Due to the falling of E_F in the antibonding region in the DOS curve (see Fig. 4) for YNi_2B_2C and YCu_2B_2C, the antibonding states appear in the corresponding charge density plots in Fig. 8. The charge density distribution between boron and carbon in all the three compounds given in Fig. 8 shows that B-C directional bonding is much stronger for YCu_2B_2C than for the other two

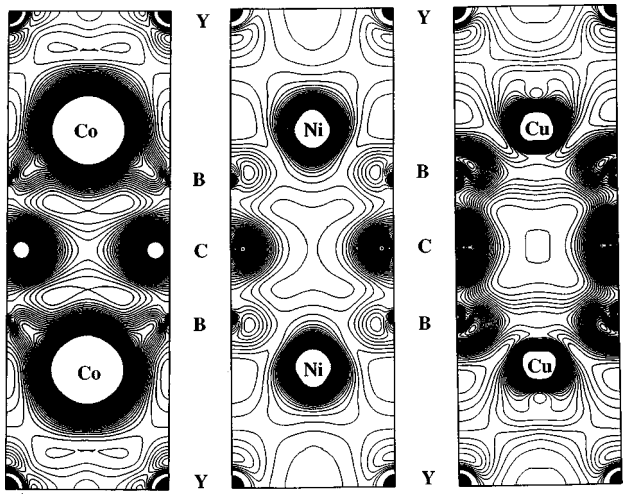

FIG. 8. The valence charge density for YT_2B_2C (T = Co.Ni,Cu) in the energy range 1 eV around Fermi level for the theoretical equilibrium volume along 100 plane. 90 contours are drawn between 0.001 and 0.05 electrons/a.u^3.

compounds. The reason is that the decreased Cu-B interaction leaves more B p states available for hybridization with C p states. Using the equilibrium volume and the c/a given in Table III the calculated transition metal-boron bond length decreases from 2.091 Å for YNi_2B_2C to 2.075 Å for YCo_2B_2C indicating that the Co substitution increases the bond strength of the tetrahedra. In contrast, the transition metal boron distance is increased to 2.114 Å for YCu_2B_2C indicating that the Cu-B bond is weaker than the Ni-B bond.

IV. ANALYSIS OF CHANGES IN T_c IN YNi_2B_2C BY Co/Cu SUBSTITUTION

To understand the microscopic origin of the changes in T_c with substitution, a knowledge about the changes in the average phonon frequency by alloying is also important. The average square of the phonon frequency $\langle\omega^2\rangle$ may be approximated by the Debye temperature through the following relation:

$$\langle\omega^2\rangle \approx 0.5\Theta_D^2. \tag{1}$$

Using this approximate relationship we have calculated the average phonon frequency. As suggested by Moruzzi, Janak, and Schwarz,[51] an approximation of the Debye temperature at the equilibrium volume can be defined at low temperatures in terms of the equilibrium bulk modulus, WS radius (r_0), and the average atomic weight (M) by

$$\Theta_D = C\left(\frac{r_0 B}{M}\right)^{1/2}. \tag{2}$$

If B is in kbar and r is in a.u. the constant C for cubic crystals is found to be 41.63. The low temperature Θ_D for YNi_2B_2C has recently been reported to be 490 K.[52] In order to match our theoretical Θ_D with this experimental value we adjust the constant C in Eq. (2) to be 45 for our tetragonal lattice and this value is used for all systems considered here. The major assumption in estimation of Θ_D using the above relation is that the shear term will not change by Co/Cu substitution in YNi_2B_2C. In order to evaluate the bulk modulus and its pressure derivative from the binding energy curve we have fitted our total energies with universal equation of states (UEOS)[53] of the form

$$P(V) = 3B_0\left(\frac{1-X}{X^2}\right)e^{\eta(1-X)}, \tag{3}$$

where $X=(V/V_0)^{1/3}$ and $\eta = 3(B_0'-1)/2$.

An alternative approach to calculate the Debye temperature from first principle studies is through the calculation of single crystal elastic constants. The θ_D may be estimated from the averaged sound velocity ν_m by the equation[54]

$$\theta_{D_p} = \frac{h}{k}\left[\frac{3n}{4\pi}\left(\frac{N_A\rho}{M}\right)\right]^{1/3}\nu_m, \tag{4}$$

where h is Planck's constant, k is Boltzmann's constant, N_A is Avogadro's number, ρ is the density, M is the molecular weight, and n is the number of atoms in the molecule. The average wave velocity ν_m in the polycrystalline material is approximately given by[54]

$$\nu_m = \left[\frac{1}{3}\left(\frac{2}{\nu_t^3}+\frac{1}{\nu_l^3}\right)\right]^{-1/3}, \tag{5}$$

where ν_l and ν_t are the longitudinal and transverse elastic wave velocity of the polycrystalline material and are obtained from Navier's equation as follows[55] (using the polycrystalline shear modulus G and the bulk modulus B):

$$\nu_l = \left[\frac{B+4G/3}{\rho}\right]^{1/2} \quad \text{and} \quad \nu_t = \left[\frac{G}{\rho}\right]^{1/2}. \tag{6}$$

The isotropic shear moduli and bulk moduli obtained from our full potential calculation gives [using Eqs. (4)–(6)] a Debye temperature for YNi_2B_2C and YCo_2B_2C of 564 and 602 K, respectively. The predicted increasing value of the Debye temperature when one goes from YNi_2B_2C to YCo_2B_2C is 38 K from the more eloborate full potential elastic constant study. The predicted increasing value of Debye temperature obtained from the simpler approach [Eq. (2)] is 21 K. This indicates the reliability of this empirical approach to predict the trend in changes of Debye temperature with substitution. Anharmonic effects in the vibrating lattice are usually described in terms of a Grüneisen constant. At low temperature it can be expressed as[51]

$$\gamma_G = -1 - \frac{V}{2}\frac{\partial^2 P/\partial V^2}{\partial P/\partial V}. \tag{7}$$

The bulk modulus for YNi_2B_2C at room temperature has been obtained recently[56] by the high pressure studies and the value was 2 Mbar. This value is found to be in good agreement with our calculated value of 1.8 Mbar. The calculated B_0 and γ_G for $YNi_{2-x}(Co/Cu)_xB_2C$ as a function of x is displayed in Fig. 9. Because of the weakening/strengthening of the lattice with Cu/Co substitution one can expect that $\partial P/\partial V$ to increase or decrease with Co/Cu substitution. This may be a possible reason for the increase of the value of γ_G with Cu substitution and the decrease with Co substitution.

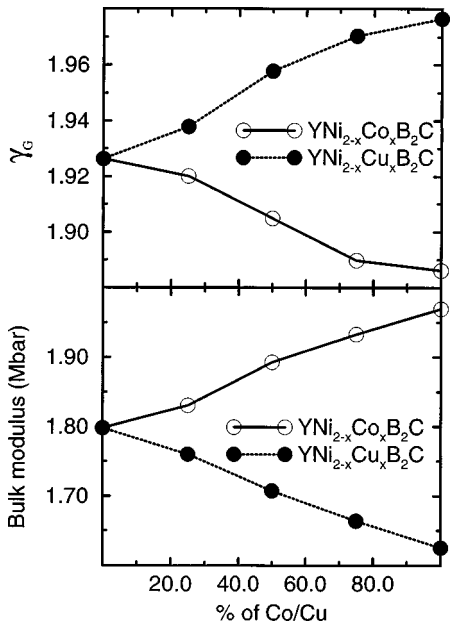

FIG. 9. The calculated bulk modulus and the Grüneisen constant for YNi_2B_2C as a function of Co/Cu substitution.

The average square of the phonon frequency and the thermodynamic Grüneisen constant are connected by the following relation;

$$\gamma_G = -\frac{\partial \ln \langle \omega^2 \rangle^{1/2}}{\partial \ln V}. \tag{8}$$

The above relation shows that γ_G will be large when $\langle \omega^2 \rangle$ and hence Θ_D is small. This is consistent with our studies in the sense that the γ_G value increases (decreases) (see Fig. 9) with Cu (Co) substitution in YNi_2B_2C and correspondingly the Θ_D value decreases (increases) as seen in Fig. 10. This figure also shows the value of the DOS at E_F, which will be discussed in Sec. V.

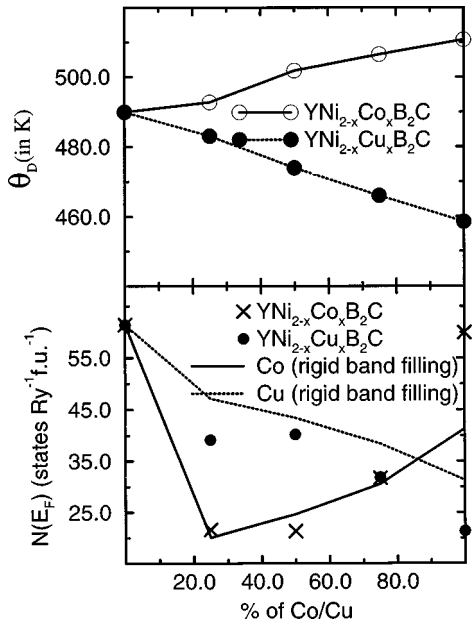

FIG. 10. The Debye temperature and density of states at the Fermi level for YNi_2B_2C as a function of Co/Cu substitution at the theoretical equilibrium volumes.

Now we will try to explain qualitatively the experimentally observed changes in T_c with Co/Cu substitution in YNi_2B_2C through our band structure results. Although we point out that this analysis is rather speculative, within the BCS limit the electron-phonon coupling constant can be expressed as[57]

$$\lambda = \frac{N(E_F)\langle I^2 \rangle}{M\langle \omega^2 \rangle}, \tag{9}$$

where the numerator is a purely electronic quantity [$N(E_F)$ is the density of states at the Fermi level and $\langle I^2 \rangle$ the average of the electron-phonon matrix elements] and the denominator is mainly a phonon term [M is the mean atomic mass and $\langle \omega^2 \rangle$ a square averaged phonon frequency which may be approximated through the Debye temperature using Eq. (1)]. If we assume that $\langle I^2 \rangle$ does not depend on substitution, the decrease in T_c may be due to two reasons: (1) Decrease of $N(E_F)$ and (2) increase of $\langle \omega^2 \rangle$ or the Debye temperature. In order to understand the variation of the Debye temperature and $N(E_F)$ as a function of Co/Cu substitution, those parameters are plotted in Fig. 10. From this figure it is clear that the $N(E_F)$ value decreases both for Co and Cu substitution in YNi_2B_2C. Moreover, the $N(E_F)$ value drops very suddenly in the low concentration range of Co in comparison with Cu. This may be one of the reasons for the experimentally observed large difference in the dT_c/dx between Co and Cu substitution.[32] Further, the Debye temperatures calculated from the bulk modulus given in Fig. 10 as a function of Co/Cu substitution increases for Co substitution and decrease for Cu substitution compared to pure Ni compound. The lattice stiffening will in general decrease the electron-phonon coupling constant through Eq. (9). Hence, apart from the decrease of $N(E_F)$, the phonon stiffening may also play an important role for the steep drop in T_c with Co substitution. In contrast, the Cu substitution softens the Debye temperature (Fig. 10). Hence, the decrease of T_c with Cu substitution is a competition by two opposite effects, such as the decrease of $N(E_F)$ and the phonon softening. As a result of the above facts, the experimentally observed dT_c/dx by Cu substitution is two times smaller than by Co substitution.

In YCo_2B_2C, our spin polarized calculation shows that the paramagnetic state is favorable in this material. Thus, we believe the magnetic correlation effect is not important for the nonappearance of superconductivity in YCo_2B_2C. The experimental susceptibility measurements show a Pauli paramagnetic behavior in this material and this is consistent with our result.[58,15] Also, the increase of the cohesive energy (Fig. 5) and the bulk modulus by an increase of the Co concentration in $YNi_{2-x}Co_xB_2C$ indicates the stiffening of the lattice. Hence the phonon stiffening may be responsible for the absence of superconductivity in YCo_2B_2C.

V. RESULTS AND DISCUSSIONS

Both Co and Cu have ionic radii of 0.72 Å compared to 0.69 Å of Ni, and hence one would expect an expansion of the YNi_2B_2C lattice by Co and Cu substitution, had it been merely a chemical pressure effect. However the experimental

x-ray diffraction measurements[32,29] show that the Co substitution leads to a lattice contraction and this is against the expectation. Our theoretically estimated equilibrium volumes as a function of Co/Cu substitution are shown in Fig. 3. From this figure we can see that the lattice expands with Cu substitution and contracts with Co substitution. This behavior is in complete agreement with recent experimental studies.[32,29] Kadowaki *et al.*[29] made systematic studies on the lattice parameter as a function of Co substitution in YNi_2B_2C and found a deviation from Vegard's law (i.e., a minimum in the unit cell volume around 25% Ni replaced by Co). They have interpreted that this anomalous behavior may be attributed to the occurrence of magnetism in this region. Interestingly, our first principles calculations also show nonlinear behavior in Fig. 3. The detailed analysis of our results shows that the anomalous behavior is not due to any magnetism and instead can be explained through simple band filling effects. In Fig. 3 the minimum in the volume is situated between 25 to 75 at. % Co substitution. Our DOS analysis shows that E_F falls on a pseudogap (i.e., all the bonding states are filled while all the antibonding states are empty) in this concentration range. In general if E_F falls in a pseudogap region is an indication of strong bonding. Hence, the anomalous behavior in the changes of the volume by Co substitution is purely a band filling effect rather than a magnetic transition. Furthermore, our spin polarized calculations also support this view point since we do not get a spontaneous onset of magnetic ordering. In binary systems, as one goes across the $3d$ series, the transition metal-boron bond strength shows a peak around Co.[59] Following this trend, as discussed by Gangopadhyay, Schuetz, and Schilling,[32] one would expect that the transition metal-boron bonds would weaken as a result of substitution for Ni with Cu, and strengthen with Co. Our charge density studies, cohesive energies, heats of formation, and Debye temperature calculations are consistent with the above expectation.

The complete replacement of Ni by Co is equivalent to a removal of two electrons/f.u and Cu replacement is equivalent to add two extra electrons/f.u in YNi_2B_2C. Hence, if we assume that the DOS curve will not change its shape by substitution (rigid band approximation), the E_F will shift to lower energy with Co substitution and higher energy with Cu substitution. In order to illustrate the validity of the rigid band approximation for $YNi_{2-x}(Co/Cu)_xB_2C$, we have plotted $N(E_F)$ obtained from the rigid band filling approximation along with the one obtained from the self-consistent supercell calculations in Fig. 10. It is interesting to note that the overall trend in the variation of $N(E_F)$ by Co/Cu substitution has been reproduced in the simple rigid band filling approximation. Apart from the trend, the absolute values of $N(E_F)$ have also been reproduced for Co substitution up to at least 75% substitution. The validity of the rigid band analysis indicates that the variation in $N(E_F)$ with substitution is mainly dominated by the shifting of E_F rather than hybridization and other chemical effects. The decrease of $N(E_F)$ by Co substitution (see Fig. 10) is larger than by Cu substitution and this trend is also consistent with the Pauli paramagnetic susceptibility obtained from normal state static magnetic susceptibility measurements.[60]

VI. SUMMARY

Based on our band structure results we have analyzed many of the trends in chemical bonding and the effect of Co/Cu substitution. In particular we conclude the following.

(1) The equilibrium volume increases (decreases) with Cu (Co) substitution in YNi_2B_2C, which is in good agreement with experimental observations. The sudden drop in volume between 25–50 % Co substitution (i.e., deviation from Vegard's law) is not due to any magnetic transition and has been explained through the band filling effect.

(2) There is strong hybridization between B-p, C-p, Ni-d, and Y-d states in YNi_2B_2C. In this compound all bonding states and some antibonding states are filled whereas, in YCo_2B_2C a small fraction of bonding states is empty.

(3) Alloying YNi_2B_2C with Co or Cu results in small changes in the electronic structure and the rigid band approximation works well. Also, the site preference of for instance Co in $Y(Ni_{1-x}Co_x)_2B_2C$ results in small changes in the total energy $\sim 0.5-10$ mRy/f.u.

(4) The use of the atomic sphere approximation works quite well for these compound, even though the structure is layered. The trend in equilibrium volume is the same in ASA as it is using a full-potential method, although the ASA volumes are somewhat too big. Moreover, the DOS obtained from both ASA and FPLMTO calculations are similar to each other.

(5) The variation of $N(E_F)$ by substitution of Ni with Co is different from that of Ni substituted by Cu in YNi_2B_2C. $N(E_F)$ decreases drastically when 25% Ni replaced by Co and afterwards increases for higher Co substitution. The $N(E_F)$ value decreases gradually with an increase of Cu concentration. The variation in $N(E_F)$ can been explained through simple rigid band filling principle.

(6) Apart from the decrease of $N(E_F)$ we speculate that the stiffening of the lattice plays an important role for sudden drop in T_c by Co substitution.

(7) The $N(E_F)$ value for nonsuperconducting YCo_2B_2C is much closer to that of superconducting YNi_2B_2C. The absence of superconductivity in YCo_2B_2C may be due to a stiffening of the lattice and/or different band filling. As our spin polarized calculation does not show any magnetic moment and the experimental studies suggest that YCo_2B_2C is Pauli paramagnetic, we believe that the suppression of superconductivity in YNi_2B_2C by Co substitution is not due to the magnetic pair breaking effect.

ACKNOWLEDGMENTS

The authors are thankful for financial support from the Swedish Natural Science Research Council and for support from the materials science consortium No. 9. P.R. is grateful to O. K. Andersen, O. Jepsen, and A. Burkhardt for providing their latest version of the TBLMTO program used in the present study and I. Abrikosov, S. Simak, and P. James for their help in evaluating ground-state properties from binding energy curves. We are also grateful to John Wills for providing us with his full-potential LMTO program and A. K. Gangopadhyay for his valuable communications prior to publication.

[1] R. Nagarajan, C. Mazumdar, Z. Hossain, S.K. Dhar, K.V. Gopalakrishnan, L.C. Gupta, C. Godart, B.D. Padalia, and R. Vijayaraghavan, Phys. Rev. Lett. **72**, 274 (1994).
[2] R.J. Cava, H. Takagi, H.W. Zandbergen, J.J. Krajewski, W.F. Peck, Jr., T. Siegrist, B. Batlogg, R.B.V. Dover, R.J. Felder, K. Mizuhashi, J.O. Lee, H. Eisaki, and S. Uchida, Nature (London) **367**, 252 (1994).
[3] T. Siegrist, H.W. Zandbergen, R.J. Cava, J.J. Krajewski, and W.F. Peck, Jr., Nature (London) **367**, 254 (1994).
[4] H.C. Ku, C.C. Lai, Y.B. You, J.H. Shieh, and W.Y. Guan, Phys. Rev. B **50**, 351 (1994).
[5] R.J. Cava, H. Takagi, B. Batlogg, H.W. Zandbergen, J.J. Krajewski, W.F. Peck, Jr., R.B.v. Dover, R.J. Felder, T. Siegrist, K. Mizuhashi, J.O. Lee, H. Eisaki, S.A. Carter, and S. Uchida, Nature (London) **367**, 146 (1994).
[6] R.J. Cava, B. Batlogg, T. Siegrist, J.J. Krajewski, W.F. Peck, Jr., S. Carter, R.J. Felder, H. Takagi, and R.B.v. Dover, Phys. Rev. B **49**, 12 384 (1994).
[7] H. Eisaki, H. Takagi, R.J. Cava, B. Batlogg, J.J. Krajewski, W.F. Peck, Jr., K. Mizuhashi, J.O. Lee, and S. Uchida, Phys. Rev. B **50**, 647 (1994).
[8] R. Nagarajan, L.C. Gupta, C. Mazumdar, Z. Hossain, S.K. Dhar, C. Godart, B.D. Padalia, and R. Vijayaraghavan, J. Alloys Compd. **225**, 571 (1995).
[9] C.V. Tomy, G. Balakrishnan, and D.M. Paul, Physica C **248**, 349 (1995).
[10] E. Brück, G.J. Nieuwenhuys, A.A. Menovsky, and J.A. Mydosh, Z. Phys. B **98**, 17 (1995).
[11] B.K. Cho, P.C. Canfield, and D.C. Johnston, Phys. Rev. B **52**, 3844 (1995).
[12] H. Eisaki, H. Takagi, R.J. Cava, B. Batlogg, J.J. Krajewski, E.F. Peck, Jr., K. Mizuhashi, J.O. Lee, and S. Uchida, Phys. Rev. B **50**, 647 (1994); H. Schmidt and H.F. Brown, Physica C **229**, 315 (1994); P.C. Canfield, B.K. Cho, D.C. Johnston, D.K. Finnemore, and M.F. Hundey, *ibid.* **230**, 397 (1994).
[13] C.V. Tomy, L.J. Chang, G. Balakrishnan, and D. Mck.Paul, Physica C **235-240**, 2551 (1994).
[14] K. Prassides, A. Lappas, M. Buchgeister, and P. Verges, Europhys. Lett. **29**, 641 (1995).
[15] G. Hilscher, H. Michor, N.M. Hong, T. Holubar, W. Perthold, M. Vybornor, and P. Rogl, Physica B **206&207**, 542 (1995).
[16] L.C. Gupta, R. Nagarajan, Z. Hossain, S.K. Dhar, R. Vijayaraghavan, C. Mazumdar, B.D. Padalia, C. Godart, and C. Levy Clement, J. Magn. Magn. Mater. **140-144**, 2053 (1995).
[17] E. Alleno, Z. Hossain, C. Godart, R. Nagarajan, and L.C. Gupta, Phys. Rev. B **52**, 7428 (1995).
[18] C.C. Lai, M.S. Lin, Y.B. You, and H.C. Ku, Phys. Rev. B **51**, 420 (1995).
[19] S.K. Dhar, R. Nagarajan, Z. Hossain, L.C. Gupta, R. Vijaraghavan, E. Tominez, and C. Godart, Solid State Commun. **98**, 985 (1996); A. Yatskar, N.K. Budraa, W.P. Beyermann, P.C. Canfield, and S.L. Bud'ko, Phys. Rev. B **54**, R3772 (1996).
[20] W.E. Pickett and D.J. Singh, Phys. Rev. Lett. **72**, 3702 (1994).
[21] L.F. Mattheiss, Phys. Rev. B **49**, 13 279 (1994).
[22] P. Ravindran, S. Sankaralingam, and R. Asokamani, Phys. Rev. B **52**, 12 921 (1995).
[23] J.I. Lee, T.S. Zhao, I.G. Kim, B.I. Min, and S.J. Youn, Phys. Rev. B **50**, 4030 (1994).
[24] L.F. Mattheiss, T. Siegrist, and R.J. Cava, Solid State Commun. **91**, 587 (1994).
[25] R.J. Cava, T. Siegrist, B. Batlogg, H. Takagi, H. Eisaki, S.A. Carter, J.J. Krajewski, and W.F. Peck, Jr., Phys. Rev. B **50**, 12 966 (1994).
[26] P.J. Jiang, M.S. Lin, J.H. Shieh, Y.B. You, H.C. Ku, and J.C. Ho, Phys. Rev. B **51**, 16 436 (1995).
[27] P. Bonville, J.A. Hodges, C. Vaast, E. Alleno, C. Godart, L.C. Gupta, Z. Hossain, and R. Nagarajan, Physica B **223-224**, 72 (1996).
[28] R. Nagarajan, L.C. Gupta, S.K. Dhar, C. Mazumdar, Z. Hossain, C. Godart, C. Levy-Clement, B.D. Padalia, and R. Vijayaraghavan, Physica B **206&207**, 548 (1995).
[29] K. Kadowaki, H. Takeya, K. Hirata, and T. Mochiku, Physica B **206&207**, 555 (1995).
[30] E.M. Baggio-Saitovitch, S.L. Bud'ko, M. Elmassalami, M.B. Fontes, J. Mondragon, W. Vanoni, and B. Giodanengo, Physica C **243**, 183 (1995).
[31] H. Schmidt, M. Müller, and H.F. Braun, Physica C **235-240**, 779 (1994).
[32] A.K. Gangopadhyay, A.J. Schuetz, and J.S. Schilling, Physica C **246**, 317 (1995).
[33] R. Coehoorn, Physica C **228**, 331 (1994).
[34] B.C. Chakoumakos and M. Paranthaman, Physica C **227**, 143 (1994).
[35] O.K. Andersen, Phys. Rev. B **12**, 3060 (1975); O.K. Andersen and O. Jepsen, Phys. Rev. Lett. **53**, 2571 (1984); O.K. Andersen, O. Jepsen, and D. Glötzel, in *Highlights of Condensed-matter Theory*, edited by F. Bassani, F. Fumi, and M.P. Tosi (North-Holland, New York, 1985); W.R.L. Lambrecht and O.K. Andersen, Phys. Rev. B **34**, 2439 (1986).
[36] P. Blöchl, O. Jepsen, and O.K. Andersen, Phys. Rev. B **49**, 16 223 (1994).
[37] J.M. Wills (unpublished); J.M. Wills and B.R. Cooper, Phys. Rev. B **36**, 3809 (1987); D.L. Price and B.R. Cooper, *ibid.* **39**, 4945 (1989).
[38] J.P. Perdew, J.A. Chevary, S.H. Vosko, K.A. Jackson, M.R. Pederson, and D.J. Singh, Phys. Rev. B **46**, 6671 (1992).
[39] D.J. Chadi and M.L. Cohen, Phys. Rev. B **8**, 5747 (1973); S. Froyen, *ibid.* **39**, 3168 (1989).
[40] D. Mayou, D. Nguyen Manh, A. Pastural, and F. Cyrot-Lackmann, Solid State Commun. **53**, 91 (1985).
[41] J.-H. Xu, T. Oguchi, and A.J. Freeman, Phys. Rev. B **35**, 6940 (1987); J.-H. Xu and A.J. Freeman, *ibid.* **40**, 11 927 (1989); **41**, 12 553 (1990); P. Ravindran, G. Subramoniam and R. Asokamani, *ibid.* **53**, 1129 (1996).
[42] D.G. Pettifor, *Bonding and Structure of Molecules and Solids* (Clarendon, Oxford, 1995).
[43] C.D. Gelatt, Jr., A.R. Williams, and V.L. Moruzzi, Phys. Rev. B **27**, 2005 (1983).
[44] P. Ravindran and R. Asokamani, Phys. Rev. B **50**, 668 (1994).
[45] P. Ravindran and R. Asokamani, J. Phys.: Condens. Matter **7**, 5567 (1995).
[46] K. Kobayashi, T. Mizokawa, K. Mamiya, A. Sekiyama, A. Fujimori, H. Takagi, H. Eisaki, S. Uchida, R.J. Cava, J.J. Krajewski, and W.F. Peck, Jr., Phys. Rev. B **54**, 507 (1996).
[47] M.S. Golden, M. Knuper, M. Kielwein, M. Buchgeister, J. Fink, D. Teehan, W.E. Pickett, and D.J. Singh, Europhys. Lett. **28**, 369 (1994).
[48] E. Pellegrin, C.T. Chen, G. Meigs, R.J. Cava, J.J. Krajewski, and W.F. Peck, Jr., Phys. Rev. B **51**, 16 159 (1995).
[49] T. Böske, M. Kielwein, M. Knupfer, S.R. Barman, G. Behr, M. Buchgeister, M.S. Golden, F. Fink, D.J. Singh, and W.E. Pickett, Solid State Commun. **99**, 23 (1996).

[50] Z. Zeng, D.E. Ellis, D. Guenzburger, and E.M. Baggio-Saitovitch, Phys. Rev. B **53**, 6613 (1996).
[51] V.L. Moruzzi, J.F. Janak, and K. Schwarz, Phys. Rev. B **37**, 790 (1988).
[52] H. Michor, T. Holubar, C. Dusek, and G. Hilscher, Phys. Rev. B **52**, 16 165 (1995).
[53] P. Vinet, J.H. Rose, J. Ferrante, and J.R. Smith, J. Phys.: Condens. Matter **1**, 1941 (1989).
[54] O.L. Anderson, J. Phys. Chem. Solids **24**, 909 (1963).
[55] E. Schreiber, O.L. Anderson, and N. Soga, *Elastic Constants and Their Measurements* (McGraw-Hill, New York, 1973).
[56] S. Meenakshi, V. Vijayakumar, R.S. Rao, B.K. Godwal, S.K. Sikka, Z. Hossain, R. Nagarajan, L.C. Gupta, and R. Vijayaraghavan, Physica B **223-224**, 93 (1996).
[57] W.L. McMillan, Physica B **167**, 331 (1968).
[58] S.L. Bud'ko, B. Giordanengo, M.B. Fontes, E.M. Baggio-Saitovitch, and A. Sulpice, Solid State Commun. **94**, 119 (1995).
[59] *CRC Hand Book of Chemistry and Physics*, 71st ed., edited by D.R. Lide (CRC, Cleveland, OH, 1991), Chaps. 9-1 to 9-5.
[60] A.K. Gangopadhyay and J.S. Schilling, Physica C **264**, 281 (1996).